Ammonia Detection using a Peptide-Based Optoelectronic Nose

Romain Dubreuil[a], Pierre Maho[a], Florine Pourtier[b], Hélène Yilmaz[b], Cyril Herrier[a], Rachid Mouflih[b], Thierry Livache[a]

[a]Aryballe, 7 rue des arts et métiers 38000 Grenoble, France
[b]HEMERA, 25 avenue du Granier 38240 Meylan, France
 r.dubreuil@aryballe.com

Ammonia is a well-known pollutant that is emitted in large quantities in the agriculture industry, largely from animal rearing. In this work, we present a new optoelectronic nose based on Mach-Zehnder interferometry using silicon technology and peptides as the sensing method. The purpose of this paper is to characterize the performance of the functionalized silicon photonics sensor by using a reference instrument based on UV spectrophotometry, provided by HEMERA. The instrument set-up used enabled a serial sampling methodology using the two devices. The gas sample was analyzed simultaneously by the optoelectronic nose and the spectrophotometer device at the same flow rate. Different concentrations of ammonia samples diluted in water were prepared and measured with this set-up. A collection of samples at different ammonia concentrations was acquired and analyzed. The results highlighted a high sensitivity (sub-ppmv) of the optoelectronic nose with respect to the ammonia concentration. The optoelectronic nose provides benefits for ammonia measurement since i/ it can be a complementary instrument to UV spectrophotometry for which common interferences are not the same ii/ it is more cost effective and compact compared to alternate reference accurate techniques iii/ it provides real-time results.

1. Introduction

The world currently produces about 175 million tons of ammonia (NH_3) per year, often for use in fertilizers, a process that is energy-intensive and produces considerable greenhouse gases. In fact, this industry is said to be responsible for approximately one to two percent of global carbon emissions, making it one of the worst on the planet (Gu, et al., 2021). When combined with nitrogen oxides and sulfur compounds produced by industrial factories and motor traffic, it causes serious damage to the environment and communities. According to the French National Research and Safety Institute, workers should not be exposed to more than 20 ppm over 15 mins (INRS, 2021).

According to literature, the use of gas sensors, such as metal oxide (Qi, et al., 2014) and polymer-based sensors (Carquigny, Sanchez, Berger, Lakard, & Lallemand, 2009), is promising for ammonia detection (Kwak, Lei, & Maric, 2019). In this work, new silicon-based functionalized sensors were used (Herrier, et al., 2022). Manufactured by Aryballe, these sensors use an array of peptides spotted on the surface (Maho, et al., 2020). They were characterized using a reference device manufactured by Hemera performing NH_3 quantification in gas phase by spectrophotometry. This device can accurately measure the amount of NH_3 in gas phase in ppmv units when using model solution – a liquid phase of ammonia and water. As it is well-known that electronic noses are very sensitive to humidity changes, a custom dilution set-up was used to stabilize the humidity of the samples during the experiments. This set-up can also perform ammonia dilution in gas phase to ensure that the multiplexed Aryballe sensor will be exposed to different concentrations of ammonia during the experiment. It is well-known in the field of electronic nose that water in gas phase generates measurable signal on the sensor. This can be tracked with a relative humidity sensor and post-treatment algorithms can distinguish the water signal from the sensor's response to the sample. In this work, we are not interested in water contribution to the signal nor humidity correction methods.

Rather, the aim of this work was to study the influence of ammonia in the range of 0-100 ppmv without the influence of water signal. To achieve this, we removed the signal due to humidity by setting a relative humidity of 40 %. Then, limit of detection was estimated to explore the potential application of such a sensor.
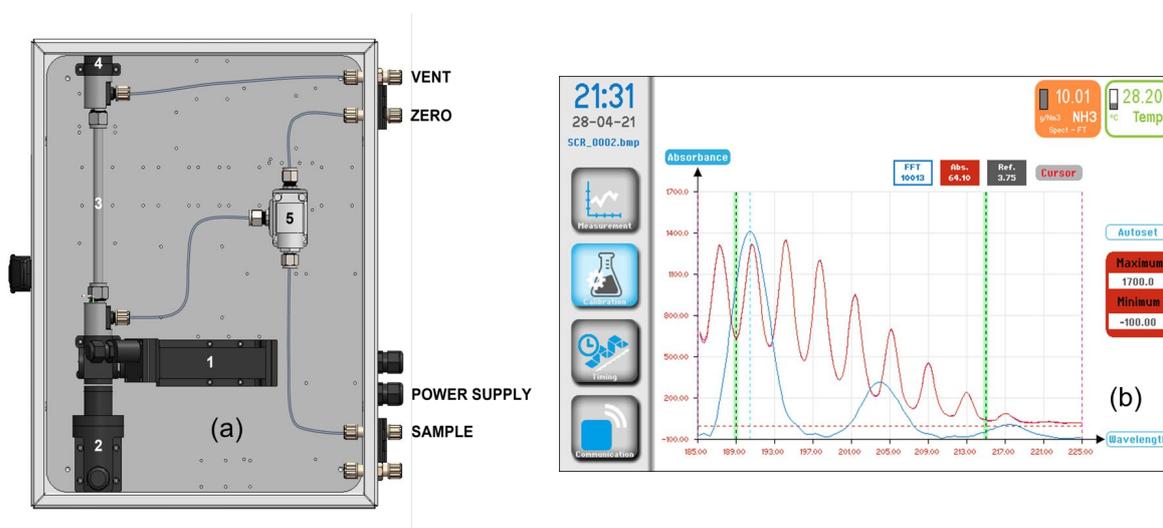

Figure 1 : HEMERA G800 device. (a): HEMERA device layout (b): NH_3 spectrum (red curve) with FFT spectrum (blue curve)

2. Materials and methods

2.1 Hemera device

After passing through the optoelectronic nose from Aryballe, the sample containing NH_3 goes through the device (model : G800) from Hemera (Meylan, France) by the sample inlet (Figure 1a). A three-way electrovalve (5) directs the fluid into the gas-cell (3) before extraction by the vent outlet. During measurement, an ultraviolet xenon lamp (2) flashes. The emitted signal is then transmitted to the spectrograph (1). The measuring principle is based on light absorption according to Beer-Lambert's law. An absorption spectrum is collected and a mathematical approach using Fast Fourier Transform (FFT) and least square calculation calculates the NH_3 concentration (Figure 1b). A mirror (4) is used to increase the optical path to detect the smallest NH_3 concentration possible. The linear range of this device is between 0 and 100 ppmv of ammonia in gas phase.

2.2. Optoelectronic nose and sample injection system

The optoelectronic nose used in this study is represented in Figure 2c (NeOse Advance (NOA) from Aryballe [1]company). More details about the instrument can be found in (Herrier, et al., 2022). The silicon sensor detects volatile compounds with an array of biosensors spotted on its surface. The signal detected from a compound depends on the interaction between the compound and these biosensors. A different intensity signal is measured for each biosensor in link with the affinity between the compound and the biosensor.
We use an automatic valve manufactured by Aryballe that allows the analysis of up to 7 samples in the same experimental run. Collection tubes are placed inside sample vials through a septum in the cap. A vent system avoids depressurization of the vial following the collection of the sample. Another tube connects to the optoelectronic nose. The duration for analysis and time between measurements is regulated to allow the headspace to adequately reform in the vials. Sensorgram in Figure 2a extracted from the signals collected shows the interaction beteen ammonia at 7 ppm and the biosensors. This instrument featured 14 different types of peptides spotted on the surface. When stimulated with the ammonia sample, the sensor response increased up to an equilibrium phase (called «plateau») on which data extraction is perfomed. The average is calculated on the most stable zone of the plateau (the red zone highlighted). Then the baseline is also calculated (from the blue zone). Signature is then calculated by subtracting the average baseline value from the average plateau value. This classical method for electronic noses provides the signature in Figure 2b.
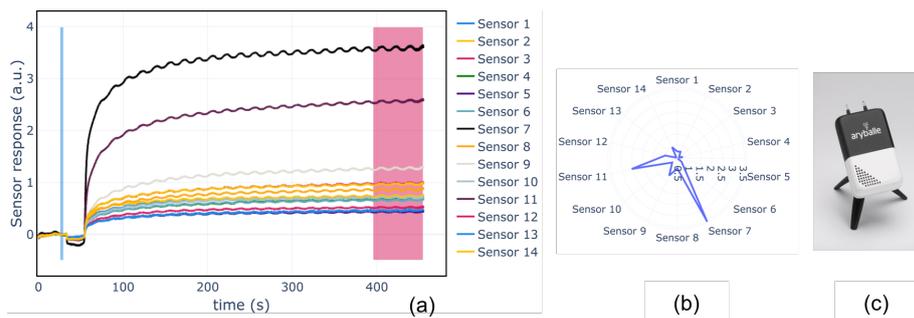
Figure 2: Optoelectronic nose and signals generated. (a) Raw signals generated by the optoelectronic nose when exposed to ammonia with the experimental set-up. Data extraction is performed by removing to the mean of the plateau at equilibrium (red zone) the mean of the baseline value (blue zone). Oscillations are due to the use of dilution valves in PWM mode, which remain even after application of a low-pass filtering. (b) Raw signature of the measurement when signal has been extracted. (c) A picture of the optoelectronic nose manufactured by Aryballe.

2.3 Dilution experimental set-up

Gas dilution using electronic valve with PWM driving system

A 12V-electronic valve from Burkert (model 6724) was used and labeled Dilution Valve 1 and Dilution Valve 2 in the set up. Briefly, this device is a 3-way valve used in medical applications. The valve is designed so that there is no direct contact between the sample and the electronics driving the valve.

A custom firmware was developed to drive the valve at PWM. Gas dilution performed with a PWM strategy has already been investigated (Andrieu, Billot, Millot, & Gharbi, 2015). The period of the dilution cycle can be set to optimize the dilution. In our experiments, a dilution cycle of 100 ms was achieved.

The experimenter can tune the opening time of the valve within a cycle by setting the percentage of time the valve is open. This achieves a simple gas dilution between the two inputs and output of the valve.

Fluidics

The set-up in represented in Figure 3a. Different samples were prepared using dilution of ammonia in water. By adjusting the amount of ammonia added to 1 mL of water, one could tune the concentration in the headspace of the solution. The first dilution valve operates a dilution of the headspace of the ammonia sample as previously described. The second dilution valve monitors the humidity of the dilution used by the first dilution valve. This second valve creates a dilution between pure water and a flask containing silica beads. This allowed accurate control of the humidity of the air going to the first dilution valve. These two valves maintained a stable relative humidity between the baseline and the analyte. The humidity sensor then evaluates the humidity value and the UV-spectrophotometer evaluates the ammonia concentration.

A sample injection involved three different steps. First, we record the baseline corresponding to the lab air measurement. In this set-up we used the valve dilution to reach a relative humidity around 40 % during baseline. Then, the analyte phase is recorded by injecting the ammonia sample. Again, the dilution valves ensured that the relative humidity is set to 40 % during the analyte period. The relative humidity was closely monitored to ensure the humidity change between the baseline and analyte measurements was no more than $\pm$ 3%. By doing so, the signal recorded was not impacted by the humidity change between the two phases. In Figure 3b, we represent an example of a measurement showing that the relative humidity is enough controlled to provide a delta value close to 0 %.

Samples

Two ammonia solutions were prepared by diluting concentrated ammonia in water (Ammonia Solution 25% from Merck KGaA). The frequency of dilution using the dilution valve directly relates to the concentration value. The sampling rate of the optoelectronic nose is set to 60 Hz and the sampling rate of the UV-spectrophotometer to 0.1 Hz. Continuous recording of ammonia – a point every 10 seconds - were obtained during the whole experiment and data were analyzed post treatment.
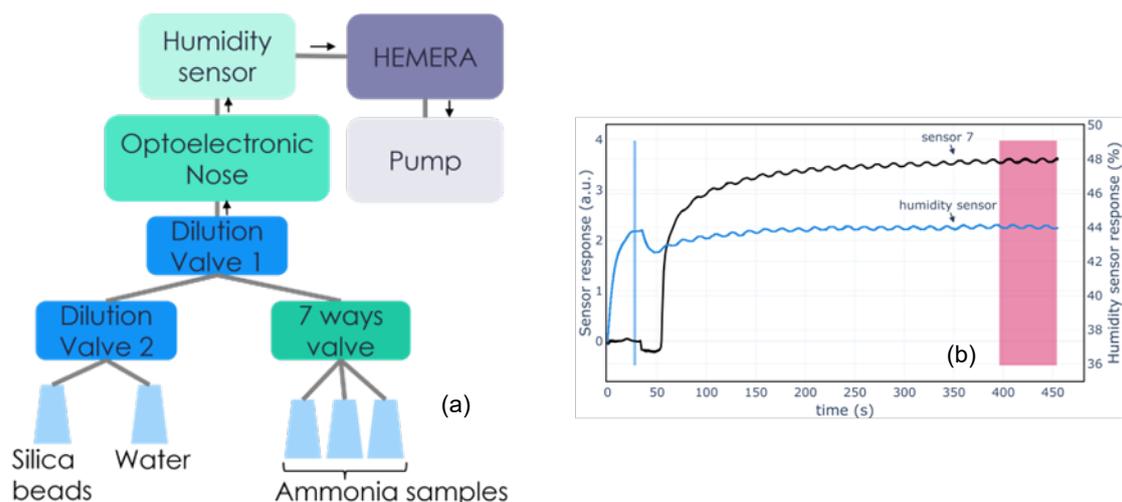
Figure 3: Experimental set-up used during the experiment. (a) Schematic of the experimental set-up built. A pump is used to create an air flow of approximatively 100 mL/min.. (b) Example of injection using this set-up. Sensor 7 shows an increase of the signal which means ammonia correctly reaches the sensor. Humidity sensors shows a fairly stable value during both baseline and plateau phase (in this example, we record a relative humidity of 43.8 % during baseline phase and a relative humidity of 44.1 % during analyte phase).

3. Theory

The sensing mechanism of the optoelectronic nose used in this study is based on adsorption process (Maho, et al., 2018). In order to model sensors' response with respect to ammonia concentration, we study two well-known adsorption isotherms, namely the Langmuir isotherm and the Freundlich isotherm.

The Langmuir isotherm (Al-Ghouti & Da'ana, 2020) is a theoretical model which describes the quantity of adsorbate on an adsorbent. The model assumes a surface containing a finite number of adsorption sites which can be occupied by a single adsorbate at a time (*i.e.* monolayer adsorption). As a consequence, the surface can reach a saturation limit where the maximum number of adsorption sites will be occupied by the adsorbate. The model is:

$$y = \frac{QKc}{1 + Kc}$$

where y stands for the sensor response at the equilibrium, Q for the sensor response when the surface is fully occupied, K for the equilibrium constant and c for the ammonia concentration. Q and K are unknown parameters where Q depends on the sensor and K depends both on the sensor and on the analyte (here, ammonia).

The Freundlich isotherm (Al-Ghouti & Da'ana, 2020), sometimes called power law in other works, is another well-known adsorption model which is more empirical. This model does not require monolayer adsorption assumption. In addition, it is applicable for a heterogeneous sensing surface, meaning that adsorption energy is not the same for all adsorption sites such that some sites may be preferred to others. The relationship between y and c is given as:

$$y = K_f c^{1/n}$$

where K_f and n are both unknown constants depending on the sensor and on the analyte. It is interesting to note that this model can be linearized as: $\log_{10}(y) = \log_{10}(K_f) + \frac{1}{n}\log_{10}(c)$. In other words, when representing $\log_{10}(y)$ with respect to $\log_{10}(c)$, a straight line should appear.

4. Results

In total, $N = 50$ measurements were captured at different concentration levels of ammonia, between 2 ppmv and 100 ppmv. This range is in the linear range of the UV-spectrophotometer. One of the challenges in this study was to keep humidity constant at two different levels, during the baseline phase and during the injection of ammonia. Throughout the study, we maintained a baseline humidity of 42.7% $\pm$ 1.7%, an analyte humidity of 42.0% $\pm$ 1.7% and a delta humidity (by subtracting the baseline humidity to the analyte humidity during a measurement) of -0.7% $\pm$ 0.8%.
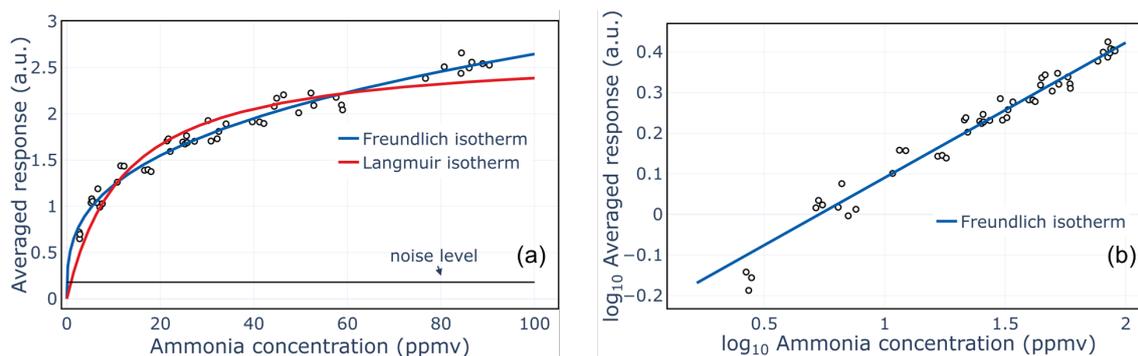
Figure 4: (a) Black points correspond to averaged responses of the optoelectronic nose at different ammonia concentration levels. These measurements have been acquired at a stable relative humidity of 40%. Red line stands for the Langmuir isotherm fitting and blue to the Freundlich isotherm fitting. (b) Representation of the measurements in log_{10}-log_{10} space showing a clear linear relationship as predicted by the Freundlich isotherm. Blue line corresponds to Freundlich isotherm in log_{10}-log_{10} space.

Concentration curve

In Figure 4a, we represent the averaged response of the optoelectronic nose with respect to ammonia concentration measured by the UV-spectrophotometer. Figure 4a highlights a clear nonlinear relationship between sensor response and ammonia concentration.

Both Langmuir and Freundlich isotherms have been fitted to the data and both describe the relationship between sensor response and ammonia concentration (see Section 3). To quantify the goodness-of-fit of each model, we calculate the root-mean-squared-error defined as:

$$RMSE = \sqrt{\frac{1}{N} \sum_{i=1}^{N} (y_i - \hat{y}_i)^2}$$

where y_i stands for the ith measurement and $\hat{y}_i$ to its prediction according one of the two models. The lower the RMSE, the better.

We found that the Freundlich isotherm ($RMSE = 0.09$) performs better than the Langmuir isotherm ($RMSE = 0.15$). In addition, in Figure 4b, we represent the measurements in log_{10}-log_{10} space to linearize the Freundlich isotherm as suggested in Section 3. Again the Freundlich model fits the data well since we report a correlation factor of 98.4% for the averaged response (the closer to 100%, the better) which indicates a strong linear relationship in log_{10}-log_{10} space as predicted by the model.

The parameter n in the Freundlich equation provides some interpretation about the adsorption mechanism at stake. If $n = 1$ then it is clear that adsorption is linear. If $n < 1$ then adsorption is a chemical process while if $n > 1$ then adsorption is a physical process (Desta, 2013). For all the sensors, n lies between 2.5 and 3.5, indicating a good physical adsorption of ammonia onto the sensors (Desta, 2013).

The better goodness-of-fit of Freundlich model can be explained as the monolayer assumption of Langmuir isotherm may be too strong for this specific case. Indeed, it is likely that the adsorption on the peptides is multilayer, such that we do not observe a saturation limit as expected by the Langmuir isotherm.

Limit of detection

The collected data did not approach the limit of detection (LOD) for the Aryballe instrument as indicated in Figure 4a. However, as the Freundlich isotherm fits the measured data, we can propose two ways to estimate the theoretical LOD.

First, we acquired nine blank measurements during which only air with no ammonia was injected. Humidity was controlled during these blank measurements such that the delta humidity between analyte and baseline phase was around $0.1\% \pm 0.8\%$. The sensor responses are extracted by subtracting the mean of baseline phase to the mean of analyte phase (see Figure 2a). These responses are then averaged to get a single value for the optoelectronic nose and we compute the noise level, noted σ, as: mean of the blank measurements + 3 x standard deviation of the blank measurements (black line in Figure 4a).

The first method to compute the LOD is to take the measurements below 10 ppmv and fit a straight line crossing the origin, giving us a slope. Then, the LOD is simply computed by dividing the noise level by the calculated slope. The theoretical LOD reaches 1.3 ppmv for the averaged response represented in Figure 4a.

However, a preliminary study after these measurements indicates that sensor response is still not linear in the range 1-10 ppmv and that the computed LOD based on a linear model is underestimated (i.e. the *real* one is less). Another albiet less conventional way to compute the LOD can be derived by using the Freundlich isotherm. The LOD is then calculated by: $e^{n(\ln \sigma - \ln K_f)}$, where n, σ and K_f are estimated from Freundlich fitting. The theoretical LOD based on this non-linear model is around 90 ppbv for the averaged response in Figure 4a, so 14 times less than the LOD based on a linear model.

5. Conclusion

This work investigated the response of an optoelectronic nose when exposed to different levels of ammonia. The set-up was adapted to cancel the contribution of water (relative humidity at 40%) on the signal using a humidity and temperature sensor combined with dilution valves. We report a good adequation of adsorption mechanism with Freundlich isotherm, a standard model used in the literature. Moreover, the theoretical LOD was estimated using different methods, leading to an estimated sub-ppmv LOD for ammonia. When trained with data as that captured in this study, it will be possible to extract ammonia levels with a fairly good accuracy - leading to semi-quantitative classification. The challenge remains with the management of humidity. Many research works suggest an increased sensitivity to ammonia when relative humidity increases (Rigoni, et al., 2017) while other works do not see a modification of their sensor response when relative humidity changes from 45 % to 90 % (Mun, Park, Lee, & Sung, 2017).. In addition, further studies will investigate the long-term reproducibility of the measurements.

Acknowledgments

References

Al-Ghouti, M. A., & Da'ana, D. A. (2020). Guidelines for the use and interpretation of adsorption isotherm models: A review. *Journal of hazardous materials*, 122383.

Andrieu, P., Billot, P., Millot, J., & Gharbi, T. (2015). Pulse Width Modulation Applied to Olfactory Stimulation for Intensity Tuning. *PLoS One*, 10,12.

Carquigny, S., Sanchez, J., Berger, F., Lakard, B., & Lallemand, F. (2009). Ammonia gas sensor based on electrosynthesized polypyrrole films. *Talanta*, 199-206.

Desta, M. B. (2013). Batch sorption experiments: Langmuir and Freundlich isotherm studies for the adsorption of textile metal ions onto Teff Straw (Eragrostis tef) agricultural waste. *Journal of Thermodynamics*, 2013:64–71.

Gu, B., Zhang, L., Van Dingenen, R., Vieno, M., Van Grinsven, H., Zhang, X., . . . Sutton, M. (2021). Abating ammonia is more cost-effective than nitrogen oxides for mitigating PM2.5 air pollution. *Science*, 374, 6568, (685-686) .

Herrier, C., Morel, N., Dubreuil, R., Liu, J., Gautheron, B., Laplatine, L., . . . Livache, T. (2022). IMAGING A SMELL – from plasmonic-based device to an array of Mach-Zehnder Interferometers. *SPIE Photonics Europe.* in press.

INRS. (2021). *https://www.inrs.fr/dms/ficheTox/FicheFicheTox/FICHETOX_16-3/FicheTox_16.pdf.*

Kwak, D., Lei, Y., & Maric, R. (2019). Ammonia gas sensors: A comprehensive review. *Talanta*, Pages 713-730.

Laplatine, L., & Herrier, C. :. (n.d.). A silicon photonic olfactory sensor based on an array of 64 bio-modified Mach-Zehnder interferometers .

Maho, P., Barthelmé, S., & Comon, P. (2018). Non-linear source separation under the Langmuir model for chemical sensors. *IEEE 10th Sensor Array and Multichannel Signal Processing Workshop (SAM)*, 380-384.

Maho, P., Herrier, C., Livache, T., Rolland, G., Comon, P., & Barthelmé, S. (2020). Reliable chiral recognition with an optoelectronic nose. *Biosensors and Bioelectronics*, 112183.

Mun, S., Park, Y., Lee, Y., & Sung, M. (2017). Highly Sensitive Ammonia Gas Sensor Based on Single-Crystal Poly(3-hexylthiophene) (P3HT) Organic Field Effect Transistor. *Langmuir*, 13554-13560.

Qi, Q., Wang, P.-P., Zhao, J., Feng, L.-L., Zhou, L.-J., Xuan, R.-F., . . . Li, G.-D. (2014). SnO2 nanoparticle-coated In2O3 nanofibers with improved NH3 sensing properties. *Sensors and Actuators B: Chemical*, 440-446.

Rigoni, F., Freddi, S., Pagliara, S., Drera, G., Sangaletti, L., Suisse, J. M., . . . Bobrinetskiy, I. (2017). Humidity-enhanced sub-ppm sensitivity to ammonia of covalently functionalized single-wall carbon nanotube bundle layers. *Nanotechnology*, 28(25):255502.